Molecular Biology of the Cell
Vol. 10, 4107–4120, December 1999

Role of Dynactin in Endocytic Traffic: Effects of Dynamitin Overexpression and Colocalization with CLIP-170

Caterina Valetti,*† Dawn M. Wetzel,‡§ Michael Schrader,‡‖ M. Josh Hasbani,‡¶ Steven R. Gill,‡# Thomas E. Kreis,* and Trina A. Schroer‡**

*Department of Cell Biology, University of Geneva, Geneva 1211, Switzerland; and ‡Department of Biology, The Johns Hopkins University, Baltimore, Maryland 21218

Submitted June 17, 1999; Accepted September 23, 1999
Monitoring Editor: Suzanne R. Pfeffer

The flow of material from peripheral, early endosomes to late endosomes requires microtubules and is thought to be facilitated by the minus end-directed motor cytoplasmic dynein and its activator dynactin. The microtubule-binding protein CLIP-170 may also play a role by providing an early link to endosomes. Here, we show that perturbation of dynactin function in vivo affects endosome dynamics and trafficking. Endosome movement, which is normally bidirectional, is completely inhibited. Receptor-mediated uptake and recycling occur normally, but cells are less susceptible to infection by enveloped viruses that require delivery to late endosomes, and they show reduced accumulation of lysosomally targeted probes. Dynactin colocalizes at microtubule plus ends with CLIP-170 in a way that depends on CLIP-170's putative cargo-binding domain. Overexpression studies using $p150^{Glued}$, the microtubule-binding subunit of dynactin, and mutant and wild-type forms of CLIP-170 indicate that CLIP-170 recruits dynactin to microtubule ends. These data suggest a new model for the formation of motile complexes of endosomes and microtubules early in the endocytic pathway.

INTRODUCTION

The microtubule cytoskeleton provides a dynamic structural framework that underlies a wide variety of subcellular motile events. The steady-state localizations of endomembrane systems such as the endoplasmic reticulum (ER), Golgi apparatus, endosomes, and lysosomes require both intact microtubules and the activities of microtubule-based motor proteins (reviewed by Goodson *et al.*, 1997). The extension of ER tubules, the Golgi-to-ER "recycling" leg of the biosynthetic pathway, and the centrifugal movement of lysosomes are thought to require the activity of a plus end-directed motor such as kinesin or a kinesin-related protein (reviewed by Lane and Allan, 1998). Cytoplasmic dynein, the predominant cytosolic minus end-directed motor, in conjunction with its activator, dynactin (Gill *et al.*, 1991), maintains the Golgi complex, endosomes, and lysosomes in the normal juxtanuclear position (Burkhardt *et al.*, 1997; Harada *et al.*, 1998). Dynein/dynactin drives membrane transport from the ER to the Golgi complex (Presley *et al.*, 1997) and may facilitate inward flow of material within the endocytic pathway, as suggested by in vitro studies of protein transfer from early to late endosomes (Bomsel *et al.*, 1990; Aniento *et al.*, 1993). However, the contributions of dynein and dynactin to endocytic trafficking in vivo have yet to be determined, because previous dynein antibody microinjection studies (Vaisberg *et al.*, 1993; Burkhardt *et al.*, 1997) and evaluation of dynein knock-out mice (Harada *et al.*, 1998) did not ad-

Present addresses: † Department of Experimental Medicine, Anatomy Section, University of Genova, Via De Toni 14, 16132 Genova, Italy; § Medical Scientist Training Program, Washington University School of Medicine, 660 S. Euclid Avenue, St. Louis, MO 63110; ‖ Institute for Cytobiology, Clinic of Philipps-University Marburg, Robert-Koch-Strasse 5, 35037 Marburg, Germany; ¶ Department of Anatomy and Neuroscience, Washington University School of Medicine, 660 S. Euclid Avenue, St. Louis, MO 63110; # The Institute for Genomic Research, 9712 Medical Center Drive, Rockville, MD 20850.

** Corresponding author. E-mail address: schroer@jhu.edu.

Abbreviations used: α_2-M, α_2-macroglobulin; Arp1, actin-related protein 1; β-gal, β-galactosidase; CMV, cytomegalovirus; DMB, dimethyl BODIPY; EEA1, early endosomal antigen 1; ER, endoplasmic reticulum; EST, expressed sequence tag; GFP, green fluorescent protein; HA, influenza hemagglutinin; LBPA, lysobisphosphatidic acid; Tfn, transferrin; TGN, *trans*-Golgi network; ts-O45-G, vesicular stomatitis virus glycoprotein, Orsay 45 temperature-sensitive strain; VEDIC, video-enhanced differential interference contrast; VEFM, video-enhanced fluorescence microscopy; VSV, vesicular stomatitis virus; VSV-G, VSV glycoprotein; wt, wild type.

dress endosome function in detail. An in-depth exploration of the effects of dynein/dynactin perturbation on endocytic trafficking and dynamics in living cells is clearly warranted.

The cytoplasmic dyneins are a multiprotein family of at least three members (Criswell *et al.*, 1996; Vaisberg *et al.*, 1996). The most abundant isoform, dynein 1, works in conjunction with a multisubunit activator protein, dynactin. Dynactin is thought to serve as an adapter that mediates dynein binding to a variety of cargo structures, including membranes, chromosomes and microtubules (reviewed by Allan, 1996; Holleran *et al.*, 1998). It is also proposed to facilitate long-range movement by increasing dynein processivity (King and Schroer, 2000). To allow for these different functions, dynactin has two distinct structural domains (Schafer *et al.*, 1994). Its rigid, filamentous backbone contains several proteins whose sequences predict both covalent and noncovalent cargo attachment mechanisms (Eckley *et al.*, 1999), whereas its flexible projecting sidearm binds dynein and microtubules (reviewed by Holleran *et al.*, 1998). These two domains are thought to be linked by the protein dynamitin which, when overexpressed, causes dynactin's sidearm to release from the backbone (Echeverri *et al.*, 1996), thus decoupling dynein-binding and cargo-anchoring functions. This leads to a variety of defects; mitotic cells arrest in pseudoprometaphase (Echeverri *et al.*, 1996), whereas interphase cells show altered steady-state distributions of the Golgi complex, endosomes, and lysosomes (Burkhardt *et al.*, 1997). Addition of excess dynamitin to cell extracts (Wittman and Hyman, 1999) and purified dynactin (Eckley *et al.*, 1999) also disrupts dynactin structure, suggesting that it can also be used to impair dynein-dependent activities in vitro. Dynamitin is thus a powerful tool for analyzing dynactin and, by inference, dynein, function in a variety of contexts.

Endosomes in the cell periphery are believed to be transiently tethered to microtubules via the cytoplasmic linker protein CLIP-170 before centripetal movement (Rickard and Kreis, 1996). CLIP-170 contributes to the binding of endosomal membranes to microtubules in vitro (Pierre *et al.*, 1992). In cells, CLIP-170 labels the growing ends of microtubules (Perez *et al.*, 1999), an appropriate site for its proposed function. Microtubule binding is regulated by phosphorylation (Rickard and Kreis, 1991), providing a means for release of CLIP-170 (and associated cargo) from microtubules under circumstances in which a static interaction is no longer needed. This might occur once motors have been recruited to the endosome–microtubule complex.

In the present study, we examine the contribution of the dynein/dynactin motor to endocytic motility and trafficking and explore its links to CLIP-170. Late endosomes located near the center of the cell move bidirectionally over long distances. In cells that overexpress dynamitin, this movement, and that of other organelles, is completely inhibited. Membranes of the endocytic pathway accumulate in the cell periphery, as seen previously. Although early and late endosomes are now in close proximity, forward traffic through the pathway is slowed. The highly conserved dynamitin N terminus is found to be sufficient to inhibit dynactin activity in vivo. In immunolocalization studies, dynactin colocalizes with CLIP-170 at microtubule plus ends, an association that depends on the CLIP-170 C-terminal cargo-binding domain. This suggests that CLIP-170 binds to microtubules first and then recruits dynactin, providing a concerted mechanism for loading endosomes onto microtubules and converting them to a motile pool.

MATERIALS AND METHODS

Cell Lines

Vero (CCL81; American Type Culture Collection, Manassas, VA) and HeLa (CCL2; American Type Culture Collection) were grown in minimum essential medium plus 1% glutamine and 5 or 10% FCS. Cos7 cells were grown in Dulbecco's modified Eagle's medium and 10% FCS.

Antibodies

Rabbit Abs were CLIP-170 (Ab 55; Pierre *et al.*, 1992), influenza hemagglutinin (HA; Daro *et al.*, 1996), MPR300 (a gift from O. Rosorius, University of Geneva), early endosomal antigen 1 (EEA1) (Simonsen *et al.*, 1998), vesicular stomatitis virus glycoprotein (VSV-G; Griffiths *et al.*, 1985), pAb p150^{Glued} (Vaughan *et al.*, 1999), and pAb dynamitin antiserum to dynamitin gel purified from bovine dynactin.

Mouse mAbs were anti-HA-epitope (Daro *et al.*, 1996), lysobisphosphatidic acid (LBPA mAb 6C4 (Kobayashi *et al.*, 1998), anti-transferrin (Tfn)-R mAb OKT9 (Sutherland *et al.*, 1981), anti-giantin (Linstedt and Hauri, 1993), mAb P5D4 against the VSV-G cytoplasmic tail (Kreis, 1986), anti-galactosyltransferase (Kawano *et al.*, 1994), anti-myc epitope mAb 9E10 (Evan *et al.*, 1985), CD63 mAb 1B5 (a gift from M. Marsh, University College, London, United Kingdom), and CLIP-170 mAbs 2D6 and 4D3 (Rickard and Kreis, 1991; Pierre *et al.*, 1992). The anti-dynamitin mAb 50A (chicken specific) and anti-p150^{Glued} mAb 150B were isolated in the same monoclonal screen that yielded mAbs 45A and 62B (Schafer *et al.*, 1994). Anti-β-galactosidase (β-gal) was from Promega (Madison, WI).

Dynamitin Cloning

A λgtll chick embryo library (B. Vennstrom, European Molecular Biology Laboratory, Heidelberg, Germany) was screened using mAb 50A. cDNAs from immunopositive clones were isolated, digested with *Eco*RI, and ligated into the *Eco*RI site of pBluescript KS II+ (Stratagene, La Jolla, CA) for later manipulations. Nested *Exo*III deletions of the longest dynamitin cDNA (1.5 kb) were sequenced using Sequenase (Amersham Life Science, Arlington Heights, IL), and the sequence from both strands was assembled using the MacDNasis DNA analysis program (Hitachi Software Engineering, San Bruno, CA).

Expression Constructs

The dynamitin cDNA insert was subcloned into two cytomegalovirus (CMV)-based expression vectors: pGW1-CMV (Quintyne *et al.*, 1999) and pCB6 containing an upstream HA tag (Balda *et al.*, 1996). To facilitate subcloning, the first 108 bp of the dynamitin cDNA was amplified by PCR using an *Alf*II site introduced at the dynamitin initiator codon and a unique, downstream *Sac*I site. The remainder of dynamitin was cloned from the *Sac*I and *Xba*I sites, and the two fragments were religated into pCB6-HA. The dynamitin N terminus (amino acids 1–87) cDNA was made by reverse transcriptase-PCR from the original λgt11 clone and subcloned in pTA (Invitrogen, Carlsbad, CA). The insert was verified by sequencing and cloned into pGW1-CMV. A λgt10 insert encoding full-length chicken p150 was cloned as described (Quintyne *et al.*, 1999). Plasmid pSG5-myc-CLIP-170 wild type (wt) contained the *Eco*RI insert from pGEM-myc-CLIP (Pierre *et al.*, 1994) subcloned into pSG5; pSG5-myc-CLIPΔ1240 was generated by truncating pSG5-myc-CLIP-170 wt using *Xho*I and *Bam*HI followed by blunting and religation (both were gifts from J. Rickard, University of Geneva). pSG5-Sar1p contained Sar1p cDNA (from B. Balch, Scripps Institute, La Jolla, CA; Aridor *et al.*, 1995)

subcloned into pSG5 (a gift from M. Gomez, University of Geneva). CMV-based vectors encoding humanized green fluorescent protein (GFP) and a red-shifted GFP (pCGFP2) were gifts from W.J. Nelson (Stanford University, Stanford, CA) and D. Shima and G. Warren (Imperial Cancer Research Fund, London, United Kingdom), respectively.

Transfection and Microinjection of Plasmids

HeLa and Vero cells, plated on 10-mm^2 coverslips 24 h before transfection, were transfected ($CaPO_4$) with Qiagen (Santa Clarita, CA)-purified plasmid DNAs (15 μg/dish) and analyzed 24–36 h later. Cos7 cells plated on 31-mm round or 22-mm^2 square coverslips 24–48 h before transfection were transfected (LipofectAMINE; Life Technologies, Gaithersburg, MD) with CsCl-purified plasmid DNAs (dynamitin, 4 μg/ml; dynamitin N terminus; GFP, 1 μg/ml) and analyzed 20–30 h later. DNA was microinjected into Vero cell nuclei using an automated microinjection system (AIS; Zeiss, Thornwood, NY) as described (Scales *et al.*, 1997). Microinjected cells were incubated at 37°C for 3–4 h before virus infection.

Virus Infection

Vero cells (36–40 h after transfection or 3–4 h after microinjection) were infected with temperature-sensitive Orsay 45 (ts-O45) VSV for 1 h at 17–20°C, 1.5 or 2 h at 20°C, or 1 or 2 h at 37°C and then incubated at the nonpermissive temperature (39.5°C) for 3 h as described (Kreis, 1986).

Immunofluorescence

Cells were fixed in −20°C methanol or 3% paraformaldehyde in PBS and then permeabilized with 0.05% saponin, or with 3.7% formaldehyde in PBS and then permeabilized with 0.1% Triton-X-100, before being stained with antibodies and observed on Zeiss Axiovert 35 or TV135 microscopes. Images were recorded as described (Pepperkok *et al.*, 1993).

Assay for Dynactin Integrity

Dynactin integrity was assayed as previously described (Echeverri *et al.*, 1996). Briefly, cells on three 10-cm dishes were transfected and grown for 30 h. Transfection efficiency was monitored by including, in each dish, a coverslip that was fixed and stained at harvest. The remaining cells were harvested using PBS-EDTA, washed, and solubilized in an equal volume of lysis buffer (Echeverri *et al.*, 1996). Cell lysates were clarified by centrifugation, the supernatants were centrifuged into sucrose gradients, and gradient fractions were analyzed on immunoblots.

Labeling with Endocytic Tracers

α_2-Macroglobulin (α_2-M; Calbiochem, La Jolla, CA) or Tfn (Sigma, St. Louis, MO) was conjugated with Cy3 or FITC/Fluor-X (Amersham) according to the manufacturer's protocol. Dye–protein conjugates were isolated on desalting columns; dye:protein ratios of 1:1.25 were obtained. Cells were incubated with Cy3-Tfn or α_2-M for analysis of probe uptake, accumulation, or motility.

Cos7 Cells. Before Tfn uptake, cells were serum starved (≥1 h at 37°C). Cells labeled with both C_5-dimethyl BODIPY (DMB)-ceramide (Molecular Probes, Eugene, OR) and Tfn were serum starved before Golgi labeling. Cells were then incubated at 37°C with Cy3-Tfn (10–15 μg/ml) for 10 min or Cy3-α_2-M (60–200 μg/ml) for 20 min. For uptake and accumulation studies, cells were rinsed for 2 min at 37°C and then fixed (Tfn and α_2-M) or chased for 90 min before fixation (α_2-M only). For each cell, labeling intensity (bright, dim, or no label) was scored, and the predominant location of fluorescence (e.g., central, random, or peripheral) was determined by eye. For motility studies, coverslips were rinsed by dipping 2 × 50 ml of 37°C HEPES-buffered medium plus 0.2% BSA before imaging.

HeLa Cells. Cells were serum starved for 1 h at 37°C in medium containing glutamine and 0.5% BSA, then labeled with 25 μg/ml FITC-Tfn for 30 min to 1 h. The coverslips were washed for 1 min and then fixed in 3% paraformaldehyde followed by −20°C methanol. Cells were labeled with Cy3-α_2M for 10–30 min, washed, and then chased for 5 min or 1 h at 37°C.

Kinetic Analysis of FITC-Tfn Cycling

To examine uptake, cells grown on coverslips were serum starved as above and then pulse labeled for 2.5, 5, 10, 20, or 60 min with 50 μg/ml FITC-Tfn. To examine recycling, coverslips were pulse labeled with 50 μg/ml FITC-Tfn for 1 h and then washed for 30 s and chased for 5, 10, 20, or 60 min in 2 ml in medium containing 10% FCS. At the end of each labeling and chase interval, coverslips were washed for 30 s and then fixed in 3% paraformaldehyde followed by −20°C methanol. Cells overexpressing dynamitin were identified using Abs the HA epitope tag. To quantify Tfn fluorescence, the cells were imaged using a charge-coupled device camera with a fixed data collection time. Images were saved as nonByte images. The periphery of each cell analyzed was defined manually. Data were analyzed using IPLab software (Scanalytics, Fairfax, VA) as described (Scales *et al.*, 1997).

Live Cell Motility Assay

For video-enhanced fluorescence microscopy (VEFM), cells were grown on 31-mm round glass coverslips. For video-enhanced differential interference contrast (VEDIC) microscopy, cells were grown on 22-mm^2 glass coverslips. The cells were transfected, stained with C_5-DMB-ceramide (Pagano *et al.*, 1991), and then loaded with endocytic tracers as above. To verify that Golgi morphology was a reliable indicator of dynamitin overexpression, cells were stained for Golgi (giantin mAb) and dynamitin (pAb dynamitin). Of 3000 cells evaluated in three separate experiments, <6% in the controls had disrupted Golgi apparatus compared with 96% of dynamitin overexpressers. Cells overexpressing GFP were identified by direct observation.

Cells in HEPES-buffered medium (without phenol red) plus 5% FCS were observed by VEDIC microscopy at room temperature. For VEFM, coverslips were mounted in 37°C medium in a heating stage (Biophysica Technologies, Towson, MD) on a Zeiss Axiovert 35TV microscope and kept covered to minimize evaporation. Temperature was monitored continuously and remained between 32 and 37°C. Cells could be kept on the microscope for longer than 2 h; particle movements continued, and the cells did not develop vacuoles or retraction fibers.

Cells exhibiting bright fluorescence were imaged through a 2× optovar using a silicon-intensified target camera (C-2500; Hamamatsu, Hamamatsu City, Japan) mounted on an intensifier (VideoScope International, Washington DC) to provide additional intensification and magnification. Data was recorded on a frame-addressable Hi8 videocassette recorder (EVO-9650; Sony, Tokyo, Japan). Video fields could be viewed continuously for several minutes with little reduction in particle motility.

Video Analysis

Particle tracks were traced from the video monitor onto transparency sheets. Run lengths and start and stop frames for each movement were used to calculate velocities. A movement was defined as a saltation at a single velocity of ≥0.3 μm. For particles undergoing multiple movements, each individual saltation was scored separately. The frustule spacing of the diatom *Pleurosigma angulatum* provided a magnification standard. Multiple coverslips were labeled with each marker, and 5–10 cells were viewed per coverslip per experiment. For analysis, cells were selected that had similar sizes and shapes. Multiple experiments were performed.

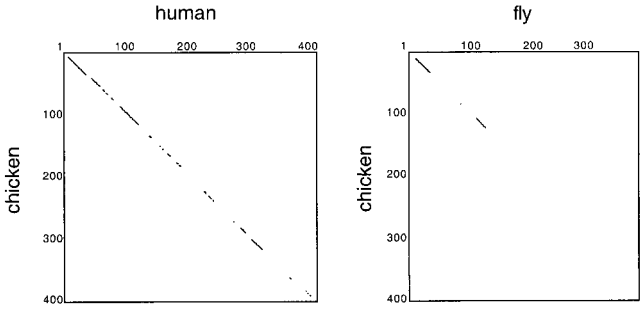

Figure 1. Homology plots of chicken versus human and fly dynamitin sequences. Plots were drawn to highlight the regions of highest homology between species. Chicken, GenBank accession number AF200744; human, accession number AAC50423; fly, for AA 1–184, EST 81725; for AA 297–380, EST AA802366, for AA 1–34 and 137–380, genomic clone AC007471.

Measurement of Endosome pH

Endosomal pH was measured using an FITC pH ratio imaging technique (Kim *et al.*, 1996). Cells overexpressing dynamitin were identified on the basis of Golgi morphology (Texas Red ceramide staining; Molecular Probes), loaded with FITC-α_2-M (0.4 mg/ml) for 20 min at 37°C, then mounted in the heating stage of the microscope. Excitation at 440 and 490 nm was provided by a xenon lamp and two monochromators (Deltascan 4000; Photon Technology International, South Brunswick, NJ). The fluorescence intensity (emission cutoff, 535 ± 20 nm) of random fields was imaged with a slow scan charge-coupled device camera (VME200A; Photometrics, Tucson, AZ) and the 490:440 ratio was calculated (Ratiotool software; Inovision, Durham, NC). At the end of each experiment, a calibration curve of fluorescence intensity versus pH was generated in situ (Kim *et al.*, 1996) and used to estimate the pH of individual fluorescent particles.

RESULTS

The Dynamitin N Terminus Is Sufficient to Perturb Dynactin Function

To identify conserved and potentially functionally important domains of dynamitin, we cloned and sequenced the chicken homologue. Its primary sequence predicts a protein of 45,052 M_r and a pI of 4.75 with 80% overall identity to the human protein. Comparison with available dynamitin sequences (human, bovine, budding yeast Jnm1p, *C. elegans* putative 37.2-kDa protein, and mouse and *Drosophila melanogaster* expressed sequence tags [ESTs]) reveals several predicted coiled coils and a possible DNA-binding motif (Echeverri *et al.*, 1996) that are conserved between species. Dynamitins show the highest similarity (97% human vs. chicken and 65% human vs. fly) in the amino-terminal region (Figure 1) and complete conservation of the first 35 amino acids among vertebrates, suggesting that this part of the protein might also be important for function.

Overexpression of dynamitin in cultured cells causes the dynein-binding p150^{Glued} sidearm to be released from the cargo-binding, actin-related protein 1 (Arp1) filament (reviewed by Allan, 1996; Schroer, 1996; Vallee and Sheetz, 1996; Holleran *et al.*, 1998). The ensuing perturbation of dynein targeting causes mitotic defects (Echeverri *et al.*, 1996) and altered endomembrane organization in interphase cells (Burkhardt *et al.*, 1997). We found membranes of the *cis*-Golgi network/Golgi apparatus (ER-Golgi intermediate compartment-positive/GFP-*N*-acetyl glucosamine transferase; our unpublished results) and *trans*-Golgi network (TGN; mannose-6-phosphate receptor-positive; Figure 2h) to be disrupted and dispersed upon overexpression of chicken dynamitin. The distributions of endocytic organelles were also altered (Figure 2), although not all endosome subcompartments were affected in the same way. Late endosomes (lysobisphosphatidic acid-positive; Figure 2d) and lysosomes (CD63-positive; our unpublished results) accumulated in clus-

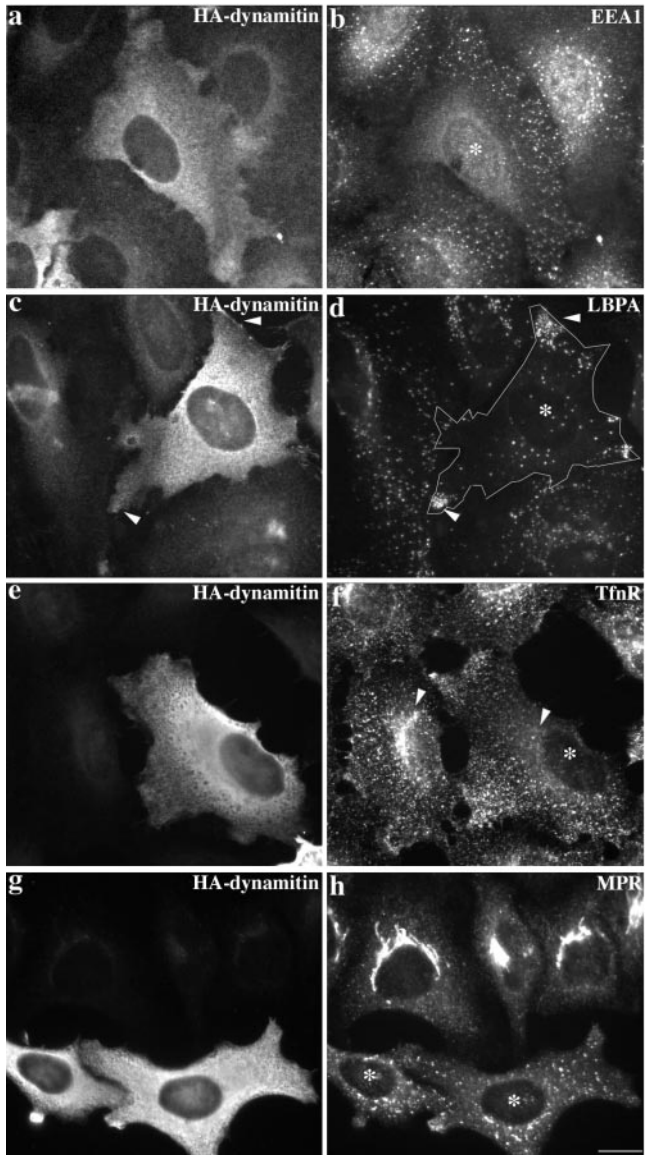

Figure 2. Effect of HA-dynamitin overexpression on the steady-state localization of early endosomes, late endosomes, and TGN. Cells were double labeled for dynamitin (HA; a, c, e, and g), early endosomes (EEA1, b; Tfn-R, f), late endosomes (LBPA; d), and TGN (MPR, mannose-6-phosphate receptor; h). Cells overexpressing HA-dynamitin are marked with asterisks. HeLa cells in a–d were fixed with 3% paraformaldehyde, and cells in e–h were fixed with MeOH. Bar, 20 μm.

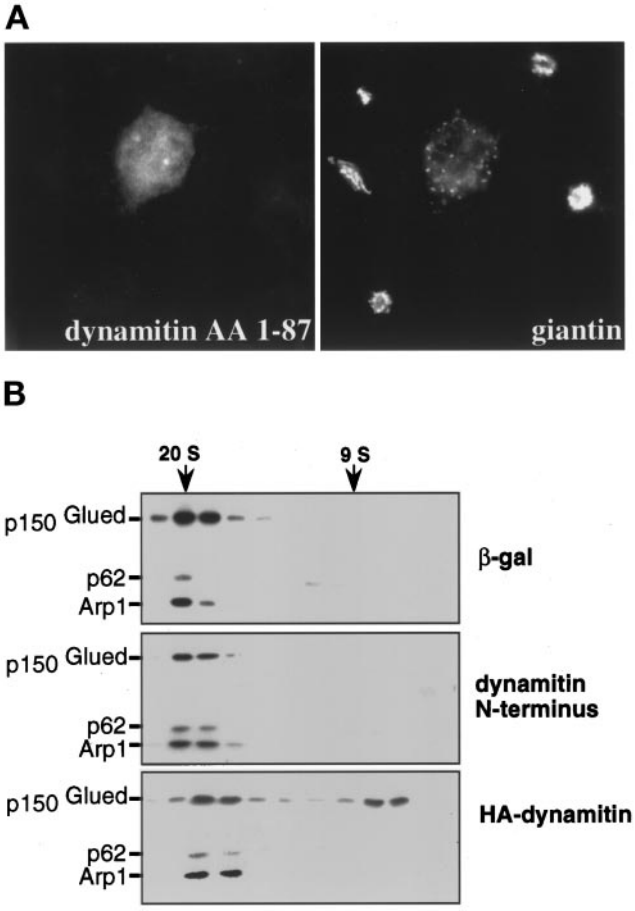

Figure 3. Dynamitin N terminus disrupts Golgi organization but not dynactin structure. (A) Cos7 cells transfected with the highly conserved dynamitin N terminus (AA 1–87) were stained for dynamitin (pAb dynamitin; left) and the Golgi complex (giantin; right). (B) Lysates of Cos7 cells transfected with β-gal, dynamitin N terminus, or HA-dynamitin were analyzed by velocity sedimentation (Echeverri *et al.*, 1996). Transfection efficiency was ≥50%. Gradient fractions were immunoblotted with antibodies to $p150^{Glued}$, p62, and Arp1. Sedimentation standards are indicated.

ters at the cell periphery. Early and recycling endosomes (positive for the early endosome antigen EEA1; Figure 2b; Tfn-R; Figure 2f) also redistributed away from the center of the cell. Some Tfn-R-labeled structures were seen at the periphery, and some appeared to be clustered, but this redistribution was not as dramatic as for late endosomes and lysosomes. In contrast, endosomes stained for EEA1 were dispersed evenly throughout the cell, which suggests a difference in the behaviors of early and recycling endosomes. No effect was detected on ER structure (calnexin-positive; our unpublished results).

Overexpression of the highly conserved N-terminal 87 amino acids of dynamitin (Figure 1) had similar disruptive effects on endosome distribution (our unpublished results) and Golgi complex organization (Figure 3A; 69% of cells; n = 675) to the full-length protein. However, sedimentation analysis of cytosolic dynactin revealed no effect on dynactin structure (Figure 3B), unlike the full-length dynamitin control (Echeverri *et al.*, 1996). Apparently, the dynamitin N terminus disrupts membrane organization without altering dynactin structure.

Dynactin Disruption Inhibits Bidirectional Organelle Movement but Not Endocytosis and Recycling

Dynamitin overexpression results in an accumulation of late endosomes and lysosomes at the cell periphery (Burkhardt *et al.*, 1997; Figure 2), whereas microtubule poisons cause these organelles to become randomly distributed. This observation led Burkhardt *et al.* (1997) to suggest that dynamitin overexpression selectively inhibits dynein-based motility but not movement driven by kinesin and other kinesin family members (the "balance of power" model for endosome and lysosome distribution). This hypothesis is supported by the observation that ER structure, which depends on ongoing plus end-directed motility, is not affected. However, other studies have shown that plus and minus end-directed movements of bidirectional particles are tightly coupled, so both are enhanced or inhibited in unison (Hamm-Alvarez *et al.*, 1993; Welte *et al.*, 1998). In our analysis, we observed that only some endosomal subcompartments were concentrated at the extreme periphery of dynamitin-overexpressing cells (Figure 2), suggesting that the balance of power model might only hold for a subset of endosomes. To gain a clearer understanding of the impact of dynamitin overexpression on bidirectional organelle motility, we turned to live cells in which the movements of endosomes and other subcellular particles could be imaged directly.

Cells were observed using VEDIC and VEFM, and the movements of two classes of organelle were quantified. Cells overexpressing dynamitin were identified by their disrupted Golgi complexes using the vital Golgi dye C_5-DMB-ceramide (Pagano *et al.*, 1991). As controls, untransfected cells, cells overexpressing cytosolic GFP, and cells in the transfected population that were not overexpressing dynamitin were examined.

Using VEDIC microscopy we analyzed the movement of the conspicuous, highly motile, cytoplasmic particles present in many fibroblasts. Nile Red staining revealed these to be lipid droplets (our unpublished results). Under normal conditions, lipid droplets undergo long- and short-range microtubule-based movements toward and away from the cell center and, on occasion, parallel to the cell margin (Hamm-Alvarez *et al.*, 1993; Bulinski *et al.*, 1997) These behaviors indicated that lipid droplets are capable of both plus end-directed and minus end-directed movement. High levels of motility were seen in untransfected cells and in the two transfection controls (Table 1). In contrast, lipid droplets in cells overexpressing dynamitin showed almost no movement. All motility was inhibited, suggesting that more than one motor had been affected. The lipid droplets did not accumulate at the cell periphery (our unpublished results) suggesting that, for these organelles, the balance of power model did not hold.

We then investigated the movement of endosomes, which are known to rely on microtubules and dynein for their steady-state distribution in vivo (Matteoni and Kreis, 1987; Burkhardt *et al.*, 1997). Microtubules and dynein also con-

Table 1. Organelle motility

Label	Column A, control (untransfected)	Column B, control (GFP)	Column C, control (transfected, not expressing)	Column D, dynamitin overexpression
None (VEDIC)	463	447	455	28
Tfn, short-range movement	176	ND	173	176
Tfn, long-range movement	36	ND	30	12
α_2-M	413	316	272	14

Motility was analyzed in Cos7 cells subjected to three conditions: no transfection (Column A), transfection with GFP (Column B), or transfection with dynamitin (Columns C and D). The cell population transiently transfected with the dynactin expression vector contained cells expressing normal levels of dynamitin (Column C, transfected, not expressing) that were used as internal controls. Cells were stained with the Golgi dye C_5-DMB-ceramide to identify dynamitin overexpressers (Column D). The predominant organelles detected by VEDIC microscopy were lipid droplets. Endosomes labeled with Cy3-Tfn or Cy3-α_2-M were analyzed by VEFM. At the end of each experiment, cells were fixed and stained for dynamitin to verify that cells with dispersed Golgi complexes indeed overexpressed dynamitin. The values listed are the total number of particle movements counted in the video field during 4 min of observation (four cells per condition, 1 min per cell). For particles containing Tfn, both short-range (0.3 to 0.5-μm) and long-range ($\geq$0.5-μm) translocations were measured. For lipid droplets and endosomes stained with α_2-M only long-range movements ($\geq$0.5-μm) were scored. ND, not determined.

tribute to endocytic trafficking and fusion in vivo and in vitro, suggesting that endosome motility might contribute to function as well as steady-state localization (Gruenberg *et al.*, 1989; Bomsel *et al.*, 1990; Aniento *et al.*, 1993). We visualized early endosomes using Tfn conjugated with the brilliantly fluorescent, photo-stable dye Cy3. Cells were briefly loaded with the probe and immediately viewed by VEFM. In control Cos7 and HeLa cells, Tfn first appeared in irregularly shaped structures (0.2–2 μm diameter) in the periphery ("sorting endosomes") and near the nucleus ("recycling endosomes"). This distribution was similar to that of endosomes stained for Tfn-R (e.g., Figure 2f; Gruenberg and Maxfield, 1995) or endosomes stained for the peripherally associated early endosomal protein EEA1 (Mu *et al.*, 1995; Figure 2b). A qualitative assessment of Tfn uptake in dynamitin overexpressers indicated that most cells had internalized the probe (Figure 4B). However, Tfn was delivered to structures that were more peripherally distributed than in controls (Figures 4A, right panel, and 5D). Although these organelles showed some overlap with late endosomes, the two compartments did not completely colocalize (Figure 4A). Quantitative analysis of the Tfn cycle in individual cells (Figure 4C) revealed that dynamitin overexpressers took up and recycled Tfn as efficiently as controls, despite the altered localization of the recycling compartment. This finding corroborates recent work in Madin–Darby canine kidney cells showing that receptor recycling can occur from early endosomes in the periphery (Sheff *et al.*, 1999).

In both control and dynamitin-overexpressing Cos7 cells, Cy3-Tfn-labeled particles exhibited mostly short-range oscillations ($<$0.5 μm; Table 1; Ghosh and Maxfield, 1995; Schrader and Schroer, unpublished results). These movements did not appear to be actomyosin based, because they were not inhibited by treatment of cells with the actin poison, latrunculin A, or the broad-spectrum myosin inhibitor butanedione monoxime (our unpublished results). Longer-range ($>$0.5-μm), presumably microtubule-based, movements were occasionally observed in control cells, but these were not common, and rarer in cells overexpressing dynamitin (Table 1).

Inhibition of Early to Late Endosome Traffic and Motility

Unlike early endosomes, late endosomes undergo robust motility that is thought to use the dynein/dynactin motor complex. To test this hypothesis directly, control and dynamitin-overexpressing Cos7 cells were loaded with Cy3-labeled α_2-M. This classic endocytic marker (Willingham and Pastan, 1978) enters cells by receptor-mediated uptake but, unlike Tfn, dissociates from its receptor in early endosomes (Yamashiro *et al.*, 1989) and is trafficked to late endosomes. At early times of observation (0–25 min) Cy3-α_2M appeared in structures that resembled those labeled with FITC-Tfn (Figure 5A, middle). After ~25 min, the fluorescent particles in control cells had a variety of sizes and shapes, including round structures (0.1–4.5 μm diameter) and branched or elongated tubules (0.7–4 μm long). These translocated over long distances (up to 6 μm) in curved or straight trajectories (motility is quantified Table 1; Schrader and Schroer, unpublished results). Although the labeled structures were most abundant in the center of the cell, they moved in all directions (inward, outward, and parallel to the cell margin), and many moved bidirectionally, suggesting that they were powered by both plus and minus end-directed motors. Motility persisted for $>$1 h.

As expected, cells overexpressing dynamitin showed a dramatically different labeling pattern from controls. After a short pulse of α_2-M, the intensity (Figure 5C, left) and morphology of labeled particles were similar to control cells, suggesting that uptake and delivery to early endosomes was unaffected. However, the labeled endosomes were either randomly distributed or concentrated at the periphery (Figure 5D), and many colocalized with early endosomes stained for EEA1 (Figure 5A). For the first hour of observation, neither the randomly distributed nor peripheral structures moved to an appreciable degree (Table 1). Importantly, outward (i.e., plus end-directed) movements were not observed. Similar effects on Cy3 α_2-M uptake, localization, and particle motility were seen in most cells overexpressing the dynamitin N terminus (our unpublished results).

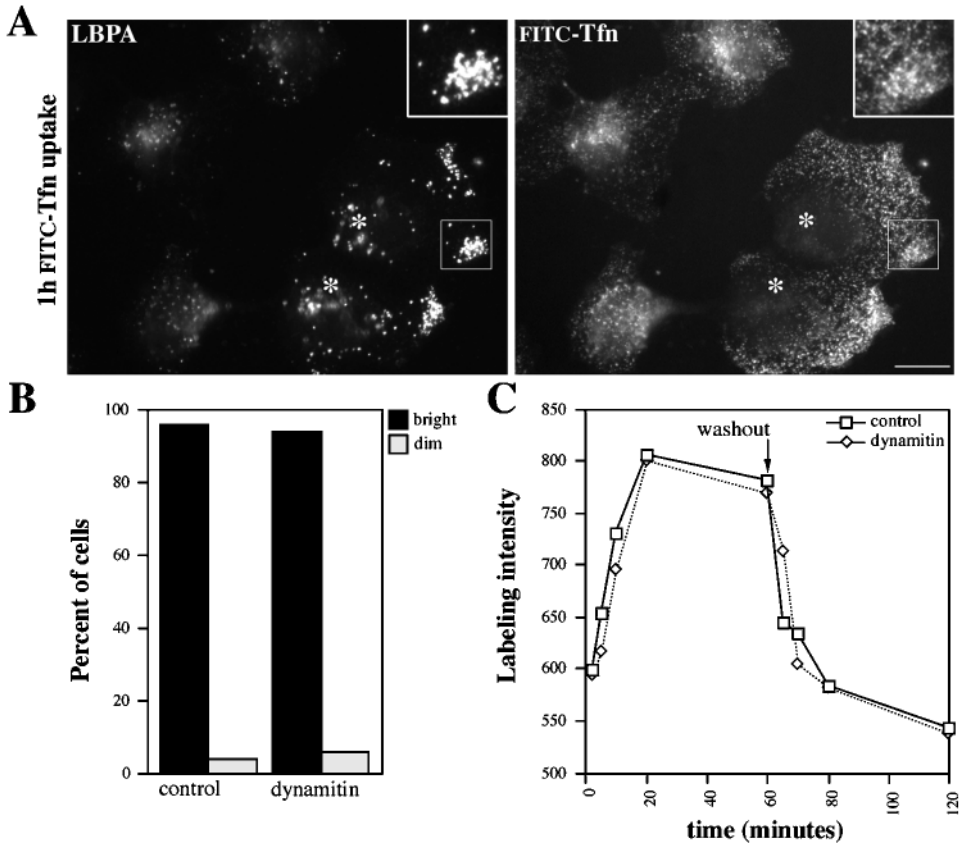

Figure 4. Tfn trafficking in control and dynamitin-overexpressing cells. (A) HeLa cells were labeled with FITC-Tfn for 1 h and then fixed (paraformaldehyde followed by MeOH) and stained for the late endosome marker LBPA (left). Inset, boxed area at 2× magnification. Cells overexpressing HA-dynamitin are marked with asterisks. (B) Qualitative analysis of uptake. Transfected Cos7 cells were labeled with Cy3-Tfn for 20 min and then fixed. Dynamitin overexpressers (i.e., cells with disrupted Golgi complexes) and control cells were scored as bright or dim (n = 180 cells total). (C) Quantitative analysis of Tfn uptake and recycling. HeLa cells were fixed after increasing times of labeling (0–60 min) or after 1 h of labeling and 0–60 min of chase. The fluorescence intensities of ≥15 control (solid lines) or dynamitin-overexpressing (dotted lines) cells were measured, and mean values are plotted. Bar in A, 20 μm.

After a 60-min chase, most dynamitin-overexpressing cells still contained detectable amounts of α_2-M, like the controls. The probe now colocalized with late endocytic markers (Figure 5B), suggesting that delivery to late endosomes had occurred. However, some cells were not labeled, and an increased percentage showed reduced levels of accumulation (Figure 5C). Because nearly all cells took up the probe originally, this finding suggested that early to late endocytic trafficking might be subtly perturbed. If traffic to late endosomes were slowed, α_2-M in early endosomes might have more opportunities to be released from the cell.

In most dynamitin-overexpressing cells Cy3-α_2-M accumulated in long-lived structures that colocalized with late endosome markers. To further characterize this compartment, we measured its lumenal pH (Figure 5E). For this analysis, cells were allowed to traffic FITC-α_2-M to late endosomes for ≥30 min. In both dynamitin-overexpressing and control cells, the labeled structures had a lumenal pH in the range of 5.0–5.5, the expected value for late endosomes. The mean pH increased slightly with increasing chase time, but the pH distribution was always the same as in controls, and the broad range of values obtained made any differences statistically insignificant. Acidification of endosomes containing α_2-M did not appear to be appreciably altered by dynamitin overexpression.

Although dynamitin overexpression has profound effects on endosome localization and motility, our findings suggest it does not dramatically alter compartment function. Cells can still take up endocytic probes and recycle them to the surface or deliver them to late endosomes with the appropriate pH. This may not be surprising, because both early and late endosomes in dynamitin-overexpressing cells are near the cell periphery, which would obviate the need for long-range movement between the two compartments. However, some cells showed reduced accumulation of α_2-M, suggesting that early-to-late endocytic traffic might be slowed. To determine the effects on trafficking of another endocytic cargo, we examined the cells' susceptibility to VSV, a virus that must be endocytosed and delivered to a low pH compartment to be infective. Virus infection is inhibited by endosome alkalization or conditions that interfere with endocytic trafficking, such as inhibition of coatomer function by mutation (Daro *et al.*, 1997) or antibody microinjection (Whitney *et al.*, 1995). For the present experiments, Vero cells were incubated with a temperature-sensitive VSV strain (ts-O45 VSV), and infection efficiency was measured by staining for newly synthesized viral glycoprotein (ts-O45-G; Figure 6A). Cells were infected at room temperature and then maintained at the restrictive temperature (39.5°C), which causes ts-O45-G to accumulate in the ER (Bergmann *et al.*, 1981). After infection for 1 h, only ~10% of Vero cells microinjected with the dynamitin expression construct showed detectable levels of ts-O45-G in the ER, compared with 80% of cells microinjected with a control vector. Cells containing dynamitin introduced by transfection were also resistant to virus infection; only ~25% of the cells had detectable levels of ts-O45-G protein expression compared with 80% of the transfection controls (Figure 6B). To deter-

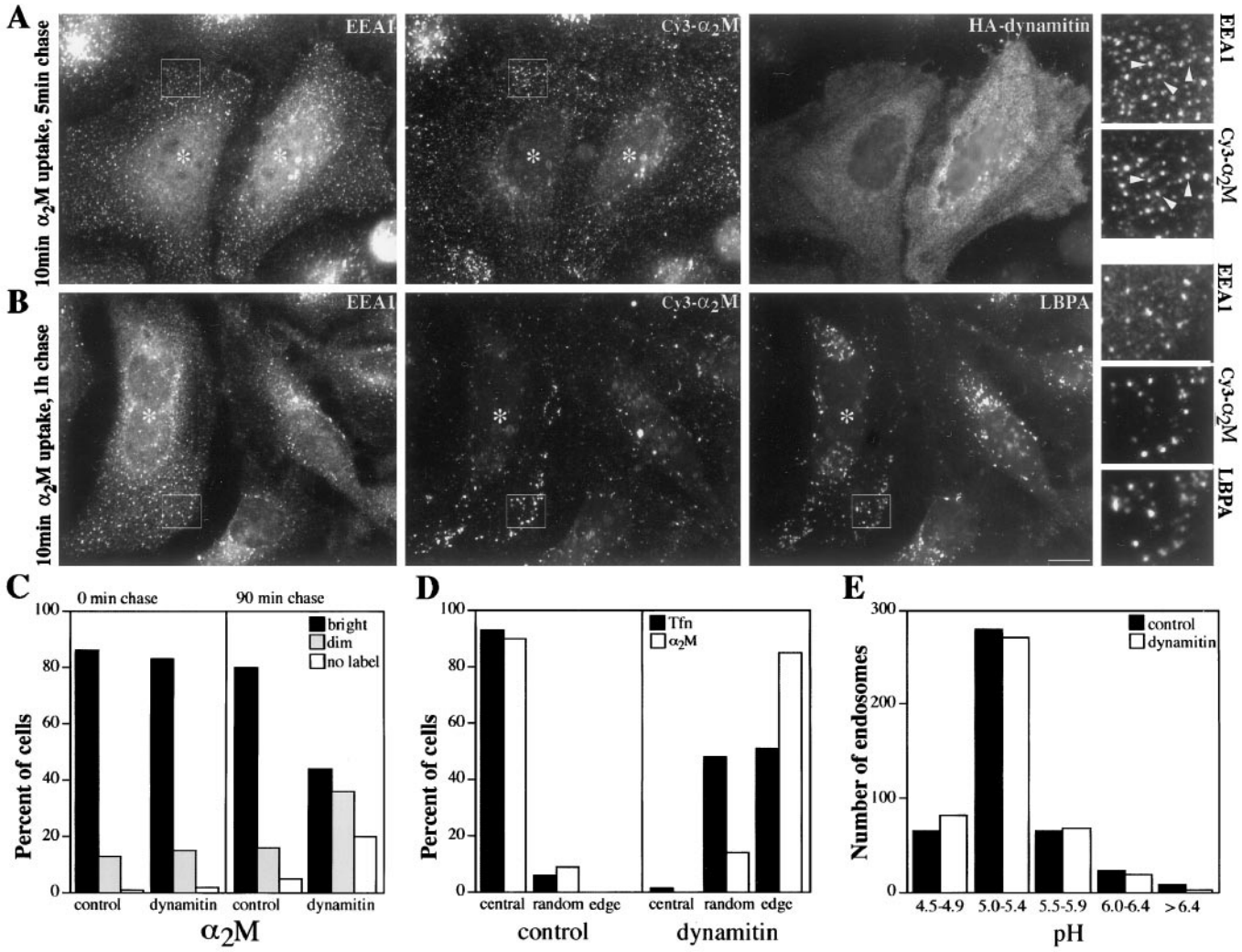

Figure 5. Analysis of endocytic trafficking in control and dynamitin-overexpressing cells. (A) HeLa cells were labeled with Cy3-α_2-M for 10 min and then chased for 5 min and fixed with paraformaldehyde. The same cells were then stained for early endosomes (EEA1; left) and overexpressed dynamitin (right); α_2-M staining is shown in the middle. (B) As in A, except the cells were chased for 1 h after the α_2-M pulse to allow the probe to traffic to late endosomes. After fixation, the cells were stained for EEA1 (left) and LBPA (right); α_2-M staining is shown in the middle. For A and B, the small panels to the right are 3× magnification views of the boxed areas; cells overexpressing HA-dynamitin are marked with asterisks. Arrows in A indicate early endosomes that also stain for α_2-M. (C) Qualitative analysis of α_2-M uptake and accumulation. Transfected Cos7 cells were labeled for 20 min and then fixed immediately (left panel) or chased for 90 min and then fixed (right panel). The fluorescence intensity (bright, dim, or no label) of ≥150 cells was assessed for each condition. (D) Subcellular distribution of endosomes loaded with Tfn or α_2-M. Transfected HeLa cells were loaded with fluorescent tracers, fixed immediately, and then scored for endosome location. Central, random, and peripheral indicate the site of the most predominant staining. Similar results were obtained in Cos7 cells (our unpublished results). (E) Analysis of endosome pH in transfected, live Cos7 cells. pH was measured by fluorescence ratio imaging (Kim *et al.*, 1996). Data were acquired from at least two different coverslips in two independent experiments. Dynamitin overexpressers were identified by staining with anti-HA (A, B, and D) or pAb dynamitin (C) or by Golgi morphology (E).

mine whether virus infection was completely blocked or just delayed, cells were infected for longer times (1.5–2 h at 20°C) or at a higher temperature (1–2 h at 37°C). Under these conditions, nearly 100% of control cells were infected. An increase (to 60–80%; Figure 6B) in infected dynamitin-overexpressing cells was also observed. This supports our hypothesis that trafficking through the endocytic pathway is delayed but not completely inhibited by dynamitin overexpression.

Association of Dynactin and CLIP-170 at Microtubule Ends

Our data verify that the dynein/dynactin motor is a major contributor to microtubule-based movement of endosomes. However, live cell imaging studies reveal that, for several minutes after entering the cell, endocytic probes in early ("sorting") endosomes remain fairly stationary and do not undergo long-range, microtubule-dependent translocations

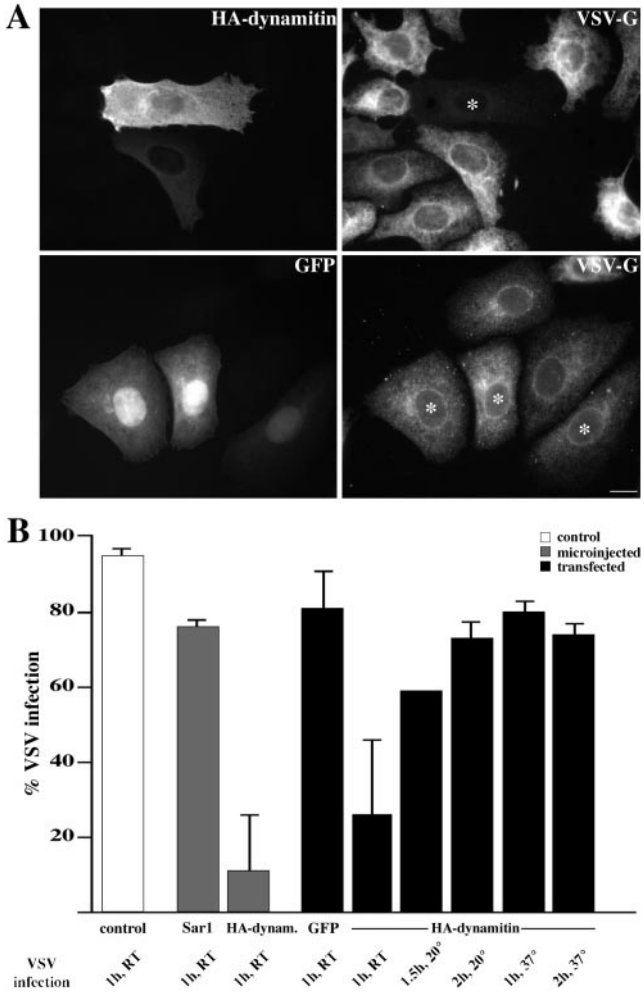

Figure 6. Effect of dynamitin overexpression on virus infection and protein export. (A) Vero cells transfected with dynamitin (top panels) or GFP (bottom panels) were infected with ts-O45 VSV for 1 h at 17–20°C and maintained at 39.5°C to retain VSV-G protein in the ER. After 3 h, cells were fixed and stained for dynamitin (HA; top left) or GFP (bottom left) and VSV-G protein (right top and bottom, mAb P5D4 and polyclonal serum). Cells overexpressing HA-dynamitin are marked with asterisks. Bar, 20 μm. (B) Quantitation of infection. Vero cells were microinjected (gray bars) with HA-dynamitin or Sar1p (a yeast rab) or transfected (black bars) with HA-dynamitin, GFP, or β-gal and infected for 1 h at room temperature (RT; 17–20°C). Control cells that received no DNA (white bar) were infected in parallel. Cells were stained, and the percent expressing both the exogenous protein and ts-O45-G protein was determined. At least 220 dynamitin-overexpressing cells, in four independent experiments, were counted for each condition. Sar1p overexpression was documented on two separate coverslips in a single experiment. The GFP bar shows data from GFP and β-gal transfections. In the remaining five black bars, cells were infected for 1 h at RT, 1.5 h at 20°C, 2 h at 20°C, 1 h at 37°C, or 2 h at 37°C.

(Ghosh and Maxfield, 1995; Schrader and Schroer, unpublished results). This delay most likely reflects the time required for the probe to transit to the appropriate endosomal subcompartment (endocytic carrier vesicle or late endosome). However, once this has occurred, an additional mechanism is required to bind the endosome to the microtubule track. CLIP-170 has been proposed to serve the initial docking role, because this protein can interact with both endosomes (Pierre *et al.*, 1992) and the distal ends of microtubules (Rickard and Kreis, 1990). Short arrays of CLIP-170 treadmill at microtubule plus ends as they grow toward the periphery (Perez *et al.*, 1999), providing a potential mechanism for attachment of peripheral endosomes and other structures (Dujardin *et al.*, 1998).

The p150^{Glued} subunit of dynactin contains a CLIP-170-related microtubule-binding motif that may contribute to dynein processivity by transiently stabilizing the enzyme–cargo link (King, and Schroer, 2000). Given the structural similarities of CLIP-170 and p150^{Glued} (Pierre *et al.*, 1992) and their overlapping roles in endosome–microtubule interactions, these two proteins may work in concert at microtubule plus ends. CLIP-170 might promote the formation of a nonmotile, microtubule–endosome complex, which would first recruit dynactin and then dynein. As a first test of this model, we compared the subcellular localizations of CLIP-170 and dynactin in HeLa cells. Previous dynactin localization studies showed a fine, punctate staining throughout the cell and accumulation at centrosomes (Gill *et al.*, 1991; Paschal *et al.*, 1993; Waterman-Storer *et al.*, 1995; Holleran *et al.*, 1996). Some of this staining colocalizes with CLIP-170 (Vaughan *et al.*, 1999). In double-labeling studies, we also observed dynactin staining that colocalized with CLIP-170 in short linear arrays in the cell periphery (Figure 7, a and b).

Both CLIP-170 and dynactin p150^{Glued} are able to bind microtubules directly via their N-terminal microtubule binding sites (Pierre *et al.*, 1992; Waterman-Storer *et al.*, 1995). According to our model, CLIP-170 binds microtubules first. To test this hypothesis, we overexpressed different dynactin subunits and determined their effects on CLIP-170 localization. If intact dynactin were required, dynamitin overexpression would be expected to alter CLIP-170 distribution. When overexpressed at low levels, dynamitin colocalized with CLIP-170 along microtubules (Figure 7, c and d). Even high-level dynamitin overexpression had no detectable effect on CLIP-170 at microtubule plus ends (Figure 7e and f), corroborating a recent report (Vaughan *et al.*, 1999). These results indicate that CLIP-170 plus end binding does not require intact dynactin.

Dynamitin overexpression causes p150^{Glued} to dissociate from dynactin's Arp1 backbone (Echeverri *et al.*, 1996). The released p150^{Glued} may still be able to interact with potential binding partners, including microtubules. In dynamitin-overexpressing cells, p150^{Glued} is still seen at microtubule ends (Vaughan *et al.*, 1999). When p150^{Glued} by itself is overexpressed in cells, it binds microtubules along their length (Waterman-Storer *et al.*, 1995; Figure 8b). CLIP-170 in these cells is still present in peripheral, linear arrays (Figure 8a), suggesting that CLIP-170 binds microtubule plus ends independently of p150^{Glued}.

Parallel experiments were performed to determine whether CLIP-170 overexpression affected dynactin localization. At low levels, overexpressed CLIP-170 forms small microtubule-associated structures (Figure 8e), and at higher levels, CLIP-170 accumulates in patchy aggregates (Figure 8c; (Pierre *et al.*, 1994). These structures also stained for dynactin subunits (p150^{Glued}, Figure 8d; Arp1, Figure 8f).

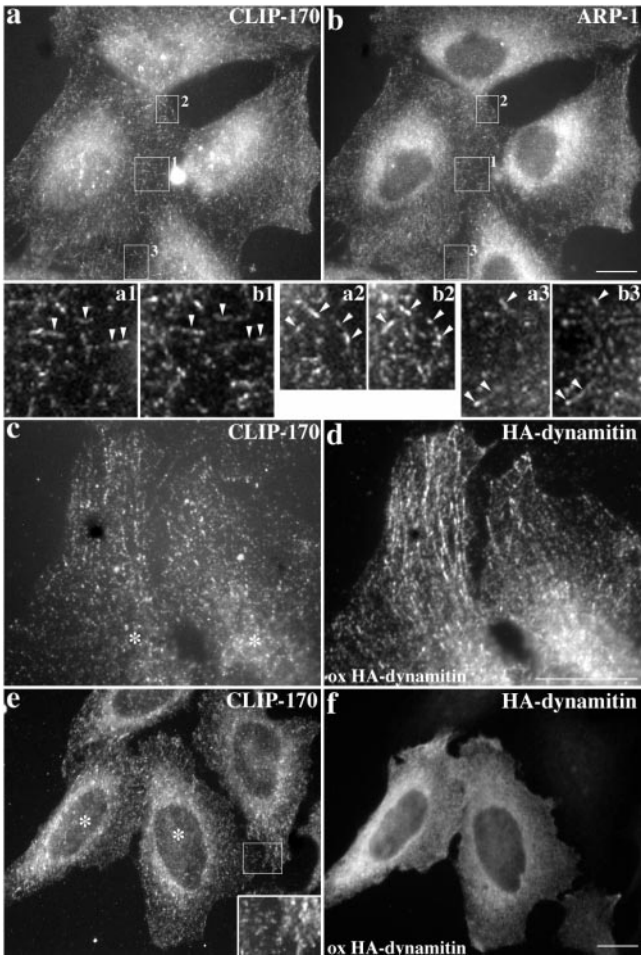

Figure 7. Effects of dynamitin overexpression on colocalization of CLIP-170 and dynactin at microtubule ends. (a and b) Control cells costained for CLIP-170 and dynactin (Arp1). (c and d) High-magnification view of two cells overexpressing dynamitin at a low level showing staining of peripheral microtubule ends. (e and f) High-level dynamitin overexpression (asterisks in e marks overexpressing cells). HeLa cells were stained for CLIP-170 (pAb 55, a; mAbs 2D6 and 4D3, c and e), dynactin (Arp1 mAb 45A, b) or dynamitin (pAb anti-HA, d and f). All were fixed with MeOH. Bars, 20 μm. Magnification in insets a1–b3, 4×.

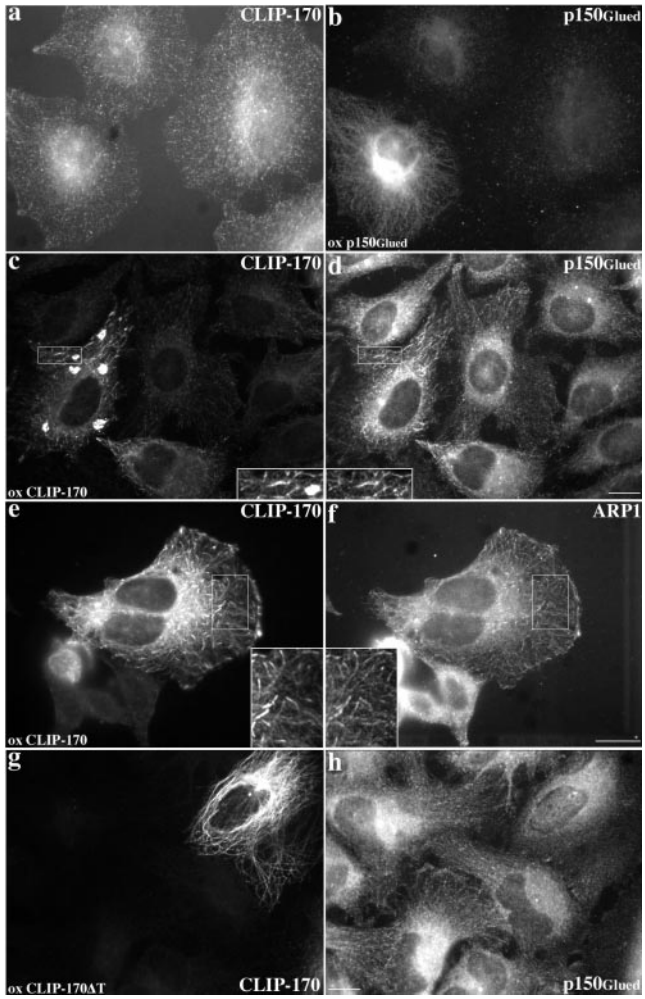

Figure 8. Effects of $p150^{Glued}$ and CLIP-170 overexpression on CLIP-170 and dynactin localization. (a and b) $p150^{Glued}$ overexpression. (c–f) Effects of wt CLIP-170 overexpression on $p150^{Glued}$ (c and d) and Arp1 (e and f) staining. (g and h) Overexpression of CLIP-170ΔT (lacking the C-terminal domain that contains the metal-binding motif). HeLa cells were stained for CLIP-170 (pAb 55, a and e; 2D6 and 4D3, c; anti-myc mAb 9E10, g) or dynactin ($p150^{Glued}$: mAb 150.1, b; pAb 150^{Glued}, d and h; Arp1: mAb 45A, f). All were fixed with MeOH. Bars, 20 μm. Inset magnifications, 2×.

The localizations of the Golgi complex, late endosomes, and lysosomes were normal in cells overexpressing CLIP-170 (Figure 9). This suggests that the actions of dynein and dynactin contribute more significantly than CLIP-170 to the final distributions of these organelles.

In addition to its microtubule-binding domain, CLIP-170 contains a metal-binding motif (Pierre *et al.*, 1992) that is implicated in cargo interactions (Pierre *et al.*, 1994; Dujardin *et al.*, 1998). Deletion of the protein domain containing this motif yields a mutant species that can still bind microtubules but does not accumulate in aggregates (Pierre *et al.*, 1994; Figure 8g). The mutant protein does not recruit dynactin (Figure 8h), suggesting that the putative cargo-binding domain is required for the interaction. Moreover, dynactin is no longer detected in linear stretches at microtubule plus ends. Quantitative determination of the prevalence of the peripheral, linear dynactin staining revealed it in nearly all of cells in the control population (97%; n = 191) but in only a minority (18%; n = 38) of those overexpressing the mutant CLIP-170 species. This reinforces the idea that CLIP-170 binds microtubule plus ends independently of dynactin and again suggests that the CLIP-170 putative metal-binding domain contributes to dynactin interactions.

DISCUSSION

Our data provide new insights into the roles of dynein, dynactin, and CLIP-170 in endosome function. The clear but limited effects of dynamitin overexpression on endocytic

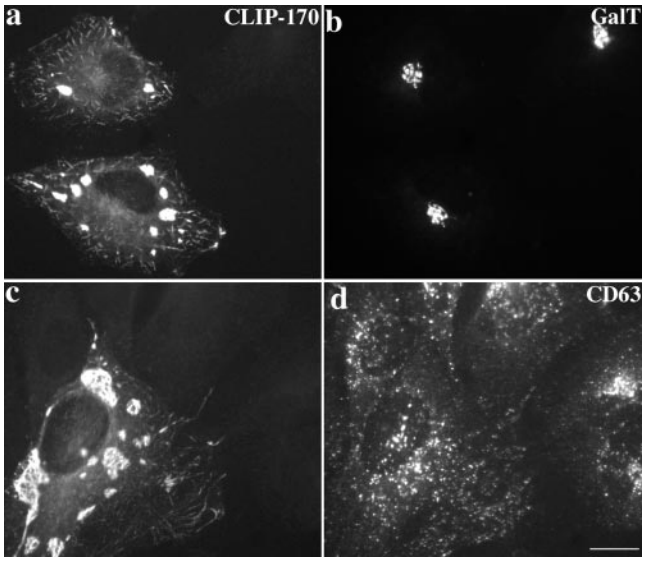

Figure 9. Effects of CLIP-170 overexpression on Golgi complex, late endosome, and lysosome distributions. HeLa cells were fixed with MeOH and stained with Abs to (a and c) CLIP-170 (pAb 55), (b) galactosyl transferase, and (d) CD63 (a LAMP family member; mAb 1B5). Bar, 20 μm.

trafficking refine our understanding of the contributions of microtubule-based movement to this process. CLIP-170 and dynactin colocalize at microtubule plus ends, and binding is found to be CLIP-170 dependent, suggesting a hierarchy of binding. We have also identified the highly conserved dynamitin N terminus as a novel potential dynein-binding element. On the basis of our findings, we propose a series of molecular interactions that may underlie endosome docking and movement. Endosome-associated CLIP-170 provides the initial link to microtubules and recruits dynactin, which then binds dynein. Once dynein is bound and/or activated, CLIP-170 releases its grip on the microtubule, and long-range endosome motility begins.

The discovery that overexpression of the dynamitin N terminus perturbs endomembrane dynamics without affecting dynactin structure was unexpected. Although p150^{Glued} is the only dynactin subunit that has been shown to bind dynein directly (reviewed by Allan, 1996; Schroer, 1996; Holleran *et al.*, 1998), our results suggest that dynamitin may also play a role. p150^{Glued} and dynamitin are tightly associated within the projecting dynactin sidearm (Eckley *et al.*, 1999) that is proposed to serve as the dynein-binding site. Dynamitin may stabilize the dynein–dynactin interaction by binding dynein directly. We find (Quintyne *et al.*, 1999) that overexpression of different dynactin subunits can have a variety of effects, including Golgi complex and endosome dispersion, disorganization of the interphase microtubule array, and disruption of dynactin structure. Dynamitin induces all these effects, whereas other dynactin subunits such as p150^{Glued} disrupt Golgi structure and microtubule organization without affecting dynactin integrity. These overexpressed dynactin subunits, as well as the p150^{Glued} released by dynamitin overexpression, most likely perturb dynactin function by competing for binding sites on dynein or cargo. The dynamitin N terminus may act in a similar manner.

We suspect that the immediate effect of dynamitin overexpression is to inhibit dynein-based movement selectively, allowing plus end-directed movement to predominate for a short time, in support of a previous hypothesis (Burkhardt *et al.*, 1997). However, we observe no plus end-directed particle movements in dynamitin-overexpressing cells, suggesting that, at steady state, kinesin and/or kinesin-related protein-based motility is also inhibited. Late endosomes and lysosomes might possess a latent microtubule plus end binding activity (e.g., CLIP-170) that would explain their microtubule-dependent retention at the periphery (Burkhardt *et al.*, 1997; Harada *et al.*, 1998). Regardless of the mechanism for endosome relocalization, our results suggest that cells overexpressing dynamitin have arrived at a new steady-state condition in which endosome movement has stopped. Under normal conditions, overall membrane flux is kept in balance so that export parallels import (Steinman *et al.*, 1976). The bidirectional movement of individual organelles (e.g., lipid droplets) is also held in balance, because motility in both directions is altered in parallel when cells are subjected to physiological (Hamm-Alvarez *et al.*, 1993) or genetic manipulation (Welte *et al.*, 1998). Endosome movements may be subject to similar controls. Current models of the mechanism underlying coordinated organelle movement invoke a shared motor receptor (Sheetz *et al.*, 1989; Vallee and Sheetz, 1996), although other mechanisms are possible. The use of dynamitin overexpression and other dynein-selective inhibitors should prove useful in further studies of this important question.

Our results suggest the additional intriguing possibility that endosome function is governed by a control mechanism that links trafficking with compartment architecture. Precedent is seen in two trafficking-defective Chinese hamster ovary cell lines that exhibit distinct endocytosis phenotypes (McGraw *et al.*, 1993; Daro *et al.*, 1997). Both show peripheral accumulations of early and late endosomes without any obvious alteration to microtubules. Similar endosome rearrangements are seen in chloroquine-treated chick embryo fibroblasts (Lippincott-Schwartz and Fambrough, personal communication). Apparently, disruption of endocytic traffic and endosome rearrangement are tightly coupled. Although the primary defect is different from cells overexpressing dynamitin (e.g., the ldlF cell line encodes a mutant ϵ-COP; Daro *et al.*, 1997), mutant Chinese hamster ovary cells show alterations in late endosome function similar to those we observe. Endocytic cargoes such as VSV (Daro *et al.*, 1997) and ricin (McGraw *et al.*, 1993) do not pass from acidic endosomal compartments to the cytoplasm, and delivery of epidermal growth factor to lysosomes is impaired (Daro *et al.*, 1997). In dynamitin-overexpressing cells and in mutant cell lines, short-range cycling of material between early endosomes and the plasma membrane continues. Late endosomal membranes may be induced to cycle in parallel when traffic is disrupted. The perturbation of normal mechanisms for forward or inward movement (e.g., budding or dynein-driven motility) might then allow the endosomal compartments participating in these loops to accumulate in the cell periphery near sites of uptake.

Early events in the endocytic pathway, such as ligand uptake and receptor recycling, are found to occur normally

in dynamitin-overexpressing cells. However, trafficking to late endosomes is slowed. Under normal conditions, microtubules have been proposed to expedite transfer of material from early to late endosomes, perhaps via endocytic carrier vesicles (Gruenberg *et al.*, 1989). Why then, in cells in which these compartments are near each other, should endocytic traffic be impaired? One possibility is that dynein-based motility is required to transport endocytic vesicles in the periphery through actin-rich cortex (Marsh and Bron, 1997). The spatial segregation that results from microtubule-based movement may also be required to maintain the distinct functions of different endocytic compartments (Gruenberg and Maxfield, 1995; Mellman, 1996). Endosomes that have been relocated to the cell periphery may fuse promiscuously with each other, which would result in membrane mixing unless balanced by sorting and retrieval mechanisms. Early and late endosome markers remain distinct in dynamitin-overexpressing cells, indicating that the two compartments are not completely randomized. However, inappropriate exchange of functionally important components or inhibitory factors not examined here might lead to the trafficking delays we observe.

Early and late endosomes are both highly pleiomorphic organelles, yet no clear relationship between structure and function has been established. The membrane deformations induced by microtubule motor activity may, in fact, contribute to membrane fusion. In pure lipid bilayer systems, high degrees of membrane curvature facilitate fusion (Chernomordik, 1996). The enhancement of early and late endosome content mixing in vitro seen in the presence of microtubules (Aniento *et al.*, 1993) may be another reflection of this phenomenon.

Whatever other roles it may play in trafficking, it is clear that the dynein/dynactin motor is critical for the translocation of endosomal membranes on microtubules. What remains an open question is how endosomes switch from the short-range, oscillatory movements seen early on to the long-range, bidirectional translocations seen at later times. The discovery that dynactin colocalizes with CLIP-170 at microtubule ends suggests an order of assembly of the microtubule–endosome complex. Microtubules extending into the periphery may contact an endosome and become docked via CLIP-170. Once the endosome is tethered in this manner, CLIP-170 can recruit dynactin. At this point, dynactin may simply provide a dynein-binding site, or it may transiently stabilize the endosome–microtubule assembly via its own cargo- and microtubule-binding sites. To switch from this stable binding configuration to one that allows motility, the CLIP-170-microtubule link must be severed, perhaps by phosphorylation. This model provides many hypotheses to be tested in future studies.

ACKNOWLEDGMENTS

We thank C. Crego and N. Jeangunat for technical assistance, Dr. M. Gomez for the microinjection studies, M. Cheng, Dr. M. Eckley, Dr. S. King, and N. Quintyne for Figure 3, and N. Quintyne for the Nile Red results. Thanks to Drs. J. Gruenberg, H.-P. Hauri, A. Helenius, A. Linstedt, M. Marsh, I. Mellman, O. Rosorius, K. Simons, and T. Suganuma for antibodies and Drs. W. Balch, M. Gomez, W.J. Nelson, J. Rickard, and G. Warren for expression vectors. We thank members of the Kreis and Schroer laboratories for helpful discussions and valuable comments on the manuscript. C.V. was supported by a European Molecular Biology Organization long-term fellowship and Telethon grant 411/bi; D.M.W. was supported by a Howard Hughes Undergraduate Summer Research Fellowship and a Johns Hopkins University Provost's Award; M.S. was supported by a grant from the Deutsche Forschungsgemeinschaft; T.E.K. was supported by the Fonds Nationale Suisse and the Canton de Genève; and T.A.S. was supported by National Institutes of Health grants GM-44589 and DK-44375 and a Lucile and David Packard Fellowship for Science and Engineering.

REFERENCES

Allan, V. (1996). Motor proteins: a dynamic duo. Curr. Biol. *6*, 630–633.

Aniento, F., Emans, N., Griffiths, G., and Gruenberg, J. (1993). Cytoplasmic dynein-dependent vesicular transport from early to late endosomes. J. Cell Biol. *123*, 1373–1387.

Aridor, M., Bannykh, S.I., Rowe, T., and Balch, W.E. (1995). Sequential coupling between COPII and COPI vesicle coats in endoplasmic reticulum to Golgi transport. J. Cell Biol. *131*, 875–893.

Balda, M.S., Whitney, J.A., Flores, C., Gonzalez, S., Cereijido, M., and Matter, K. (1996). Functional dissociation of paracellular permeability and transepithelial electrical resistance and disruption of the apical-basolateral intramembrane diffusion barrier by expression of a mutant tight junction membrane protein. J. Cell Biol. *134*, 1031–1049.

Bergmann, J.E., Tokuyasu, K.T., and Singer, S.J. (1981). Passage of an integral membrane protein, the vesicular stomatitis virus glycoprotein, through the Golgi apparatus en route to the plasma membrane. Proc. Natl. Acad. Sci. USA *78*, 1746–1750.

Bomsel, M., Parton, R., Kuznetsov, S.A., Schroer, T.A., and Gruenberg, J. (1990). Microtubule- and motor-dependent fusion in vitro between apical and basolateral endocytic vesicles from MDCK cells. Cell *62*, 719–731.

Bulinski, J.C., McGraw, T.E., Gruber, D., Nguyen, H.L., and Sheetz, M.P. (1997). Overexpression of MAP4 inhibits organelle motility and trafficking in vivo. J. Cell Sci. *110*, 3055–3064.

Burkhardt, J.K., Echeverri, C.J., Nilsson, T., and Vallee, R.B. (1997). Overexpression of the dynamitin (p50) subunit of the dynactin complex disrupts dynein-dependent maintanance of membrane organelle distribution. J. Cell Biol. *139*, 469–484.

Chernomordik, L. (1996). Nonbilayer lipids and biological fusion intermediates. Chem. Phys. Lipids *81*, 203–213.

Criswell, P.S., Ostrowski, L.E., and Asai, D.J. (1996). A novel cytoplasmic dynein heavy chain: expression of DHC1b in mammalian ciliated epithelial cells. J. Cell Sci. *109*, 1891–1898.

Daro, E., Sheff, D., Gomez, M., Kreis, T., and Mellman, I. (1997). Inhibition of endosome function in CHO cells bearing a temperature-sensitive defect in the coatomer (COPI) component ϵ-COP. J. Cell Biol. *139*, 1747–1759.

Daro, E., van der Sluijs, P., Galli, T., and Mellman, I. (1996). Rab4 and cellubrevin define different early endosome populations on the pathway of transferrin receptor recycling. Proc. Natl. Acad. Sci. USA *93*, 9559–9564.

Dujardin, D., Wacker, U.I., Moreau, A., Schroer, T.A., Rickard, J.E., and De Mey, J.R. (1998). Evidence for a role of CLIP-170 in the establishment of metaphase chromosome alignment. J. Cell Biol. *141*, 849–862.

Echeverri, C.J., Paschal, B.M., Vaughan, K.T., and Vallee, R.B. (1996). Molecular characterization of 50 kDa subunit of dynactin reveals function for the complex in chromosome alignment and spindle organization during mitosis. J. Cell Biol. *132*, 617–633.

Eckley, D.M., Gill, S.R., Melkonian, K.M., Bingham, J.B., Melkonian, K.M., Goodson, H.V., Heuser, J.E., and Schroer, T.A. (1999). Analysis of dynactin subcomplexes reveals a novel actin-related protein associated with the Arp1 filament pointed end. J. Cell Biol. *147*, 307–319.

Evan, G.I., Lewis, G.K., Ramsay, G., and Bishop, J.M. (1985). Isolation of monoclonal antibodies specific for human c-myc proto-oncogene product. Mol. Cell. Biol. *5*, 3610–3616.

Ghosh, R.N., and Maxfield, F.R. (1995). Evidence for nonvectorial, retrograde transferrin trafficking in the early endosomes of HEp2 cells. J. Cell Biol. *128*, 549–561.

Gill, S.R., Schroer, T.A., Szilak, I., Steuer, E.R., Sheetz, M.P., and Cleveland, D.W. (1991). Dynactin, a conserved, ubiquitously expressed component of an activator of vesicle motility mediated by cytoplasmic dynein. J. Cell Biol. *115*, 1639–1650.

Goodson, H.V., Valetti, C., and Kreis, T.E. (1997). Motors and membrane traffic. Curr. Opin Cell Biol. *9*, 18–28.

Griffiths, G., Pfeiffer, S., Simons, K., and Matlin, K. (1985). Exit of newly synthesized membrane proteins from the trans cisterna of the Golgi complex to the plasma membrane. J. Cell Biol. *101*, 949–964.

Gruenberg, J., Griffiths, G., and Howell, K.E. (1989). Characterization of the early endosome and putative endocytic carrier vesicles in vivo and with an assay of vesicle fusion in vitro. J. Cell Biol. *108*, 1301–1316.

Gruenberg, J., and Maxfield, F.R. (1995). Membrane transport in the endocytic pathway. Curr. Opin. Cell Biol. *7*, 552–563.

Hamm-Alvarez, S.F., Kim, P.Y., and Sheetz, M.P. (1993). Regulation of vesicle transport in CV-1 cells and extracts. J. Cell Sci. *106*, 955–966.

Harada, A., Takei, Y., Kanai, Y., Tanaka, Y., Nonaka, S., and Hirokawa, N. (1998). Golgi vesiculation and lysosome dispersion in cells lacking cytoplasmic dynein. J. Cell Biol. *141*, 51–59.

Holleran, E.A., Karki, S., and Holzbaur, E.L. (1998). The role of the dynactin complex in intracellular motility. Int. Rev. Cytol. *182*, 69–109.

Holleran, E.A., Tokito, M.K., Karki, S., and Holzbaur, E.L.F. (1996). Centractin (Arp1) associates with spectrin revealing a potential mechanism to link dynactin to intracellular organelles. J. Cell Biol. *135*, 1815–1829.

Kawano, J., Ide, S., Oinuma, T., and Suganuma, T. (1994). A protein-specific monoclonal antibody to rat liver beta 1→4 galactosyltransferase and its application to immunohistochemistry. J. Histochem. Cytochem. *42*, 363–369.

Kim, J.H., Lingwood, C.A., Williams, D.B., Furuya, W., Manolson, M.F., and Grinstein, S. (1996). Dynamic measurement of the pH of the Golgi complex in living cells using retrograde transport of the verotoxin receptor. J. Cell Biol. *134*, 1387–1399.

King, S.S., and Schroer, T.A. (2000). Dynactin enhances the processivity of the cytoplasmic dynein motor. Nat. Cell Biol. (*in press*).

Kobayashi, T., Stang, E., Fang, K., de Moerloose, P., Parton, R., and Gruenberg, J. (1998). A lipid associated with the antiphospholipid syndrome regulates endosome structure and function. Nature *392*, 193–197.

Kreis, T.E. (1986). Microinjected antibodies against the cytoplasmic domain of vesicular stomatitis virus glycoprotein block its transport to the cell surface. EMBO J. *5*, 931–941.

Lane, J., and Allan, V. (1998). Microtubule-based membrane movement. Biochim. Biophys. Acta *1376*, 27–55.

Linstedt, A.D., and Hauri, H.P. (1993). Giantin, a novel conserved Golgi membrane protein containing a cytoplasmic domain of at least 350 kDa. Mol. Biol. Cell *4*, 679–693.

Marsh, M., and Bron, R. (1997). SFV infection in CHO cells: cell-type specific restrictions to productive virus entry at the cell surface. J. Cell Sci. *110*, 95–103.

Matteoni, R., and Kreis, T.E. (1987). Translocation and clustering of endosomes and lysosomes depends on microtubules. J. Cell Biol. *105*, 1253–1265.

McGraw, T.E., Dunn, K.W., and Maxfield, F.R. (1993). Isolation of a temperature-sensitive variant Chinese hamster ovary cell line with a morphologically altered endocytic recycling compartment. J. Cell. Physiol. *155*, 579–594.

Mellman, I. (1996). Endocytosis and molecular sorting. Annu. Rev. Cell Dev. Biol. *12*, 575–625.

Mu, F., Callaghan, J., Steele-Mortime, R.O., Stenmark, H., Parton, R., Campbell, P., McCluskey, J., Yeo, J., Tock, E., and Toh, B. (1995). EEA1, an early endosome-associated protein. EEA1 is a conserved alpha-helical peripheral membrane protein flanked by cysteine "fingers" and contains a calmodulin-binding IQ motif. J. Biol. Chem. *270*, 13503–13511.

Pagano, R.E., Martin, O.C., Kang, H.C., and Haugland, R.P. (1991). A novel fluorescent ceramide analog for studying membrane traffic in animal cells: accumulation at the Golgi apparatus results in altered spectral properties of the sphingolipid precursor. J. Cell Biol. *113*, 1267–1279.

Paschal, B.M., Holzbaur, E.L.G., Pfister, K.K., Clark, S., Meyer, D.I., and Vallee, R.B. (1993). Characterization of a 50-kDa polypeptide in cytoplasmic dynein preparations reveals a complex with $p150^{GLUED}$ and a novel actin. J. Biol. Chem. *268*, 15318–15323.

Pepperkok, R., Scheel, J., Horstmann, H., Hauri, H.P., Griffiths, G., and Kreis, T.E. (1993). Beta-COP is essential for biosynthetic membrane transport from the endoplasmic reticulum to the Golgi complex in vivo. Cell *74*, 71–82.

Perez, F., Diamantopoulos, G.S., Stalder, R., and Kreis, T.E. (1999). CLIP-170 highlights growing microtubule ends in vivo. Cell *96*, 517–527.

Pierre, P., Pepperkok, R., and Kreis, T.E. (1994). Molecular characterization of two functional domains of CLIP-170 in vivo. J. Cell Sci. *107*, 1909–1920.

Pierre, P., Scheel, J., Rickard, J., and Kreis, T.E. (1992). CLIP-170 links endocytic vesicles to microtubules. Cell *70*, 887–900.

Presley, J.F., Zaal, K.J.M., Schroer, T.A., Cole, N.B., and Lippincott-Schwartz, J. (1997). ER to Golgi transport visualized in living cells. Nature *389*, 81–85.

Quintyne, N.J., Gill, S.R., Eckley, D.M., Crego, C.L., Compton, D.A., and Schroer, T.A. (1999). Dynactin is required for microtubule anchoring at centrosomes. J. Cell Biol. *147*, 321–334.

Rickard, J.E., and Kreis, T.E. (1990). Identification of a novel nucleotide-sensitive microtubule-binding protein in HeLa cells. J. Cell Biol. *110*, 1623–1633.

Rickard, J.E., and Kreis, T.E. (1991). Binding of pp170 to microtubules is regulated by phosphorylation. J. Biol. Chem. *266*, 17597–17605.

Rickard, J.E., and Kreis, T.E. (1996). CLIPs for organelle-microtubule interactions. Trends Cell Biol. *6*, 178–183.

Scales, S.J., Pepperkok, R., and Kreis, T.E. (1997). Visualization of ER-to-Golgi transport in living cells reveals a sequential mode of action for COPII and COPI. Cell *90*, 1137–1148.

Schafer, D.A., Gill, S.R., Cooper, J.A., Heuser, J.E., and Schroer, T.A. (1994). Ultrastructural analysis of the dynactin complex: An actin-related protein is a component of a filament that resembles f-actin. J. Cell Biol. *126*, 403–412.

Schroer, T.A. (1996). Structure and function of dynactin. Semin. Cell Biol. *7*, 321–328.

Sheetz, M.P., Steuer, E.R., and Schroer, T.A. (1989). The mechanism and regulation of fast axonal transport. Trends Neurosci. *12*, 474–478.

Sheff, D.R., Daro, E.A., Hull, M., and Mellman, I. (1999). The receptor recycling pathway contains two distince populations of early endosomes with different sorting functions. J. Cell Biol. *145*, 123–129.

Simonsen, A., Lippe, R., Christoforidis, S., Gaullier, J., Brech, A., Callaghan, J., Toh, B., Murphy, C., Zerial, M., and Stenmark, H. (1998). EEA1 links PI(3)K function to Rab5 regulation of endosome fusion. Nature *394*, 494–498.

Steinman, R.M., Brodie, S.E., and Cohn, Z.A. (1976). Membrane flow during pinocytosis. A stereologic analysis. J. Cell Biol. *68*, 665–687.

Sutherland, R., Delia, D., Schneider, C., Newman, R., Kemshead, J., and Greaves, M. (1981). Ubiquitous cell-surface glycoprotein on tumor cells is proliferation-associated receptor for transferrin. Proc. Natl. Acad. Sci. USA *78*, 4515–4519.

Vaisberg, E.A., Grissom, P.M., and McIntosh, J.R. (1996). Mammalian cells express three distinct dynein heavy chains that are localized to different cytoplasmic organelles. J. Cell Biol. *133*, 831–842.

Vaisberg, E.A., Koonce, M.P., and McIntosh, J.R. (1993). Cytoplasmic dynein plays a role in mammalian mitotic spindle formation. J. Cell Biol. *123*, 849–858.

Vallee, R.B., and Sheetz, M.P. (1996). Targeting of motor proteins. Science *271*, 1539–1544.

Vaughan, K.T., Tynan, S.H., Faulkner, N.E., Echeverri, C.J., and Vallee, R.B. (1999). Colocalization of cytoplasmic dynein with dynactin and CLIP-170 at microtubule distal ends. J. Cell Sci. *112*, 1437–1447.

Waterman-Storer, C.M., Karki, S., and Holzbaur, E.L. (1995). The $p150^{Glued}$ component of the dynactin complex binds to both microtubules and the actin-related protein centractin (Arp-1). Proc. Natl. Acad. Sci. USA *92*, 1634–1638.

Welte, M.A., Gross, S.P., Postner, M., Block, S.M., and Wieschaus, E.F. (1998). Developmental regulation of vesicle transport in *Drosophila* embryos: forces and kinetics. Cell *92*, 547–557.

Whitney, J.A., Gomez, M., Sheff, D., Kreis, T.E., and Mellman, I. (1995). Cytoplasmic coat proteins involved in endosome function. Cell *83*, 703–713.

Willingham, M.C., and Pastan, I. (1978). The visualization of fluorescent proteins in living cells by video intensification microscopy (VIM). Cell *14*, 501–507.

Wittman, T., and Hyman, A. (1999). Recombinant p50/dynamitin as a tool to examine the role of dynactin in intracellular processes. In: Methods in Cell Biology, ed. C. Rieder, San Diego: Academic Press, 137–143.

Yamashiro, D.J., Borden, L.A., and Maxfield, F.R. (1989). Kinetics of α2-macroglobulin endocytosis and degradation in mutant and wild-type Chinese hamster ovary cells. J. Cell. Physiol. *139*, 377–382.